This article has been accepted for publication in a future issue of this journal, but has not been fully edited. Content may change prior to final publication. Citation information: DOI 10.1109/TSG.2016.2645600, IEEE Transactions on Smart Grid

Control of Grid Tied Smart PV-DSTATCOM System using an Adaptive Technique

Bhim Singh, *Fellow, IEEE,* Maulik Kandpal and Ikhlaq Hussain, *Member, IEEE*

***Abstract*— This paper presents a control of smart PV (Photovoltaic)-DSTATCOM (Distribution Static Compensator) grid tied system using an adaptive reweighted zero attracting (RZA) control algorithm with P & O (Perturb and Observe) maximum power point tracking technique for a three phase system to improve power quality and support the three phase AC grid by supplying power both to the grid and the connected loads. The proposed PV grid tied system is capable of working round the clock. During sunshine conditions, the proposed system performs dual functions of improving power quality by working as DSTATCOM and also transfers power to the load and the grid obtained from PV array. However, during night or cloudy conditions, the proposed system works as DSTATCOM improving power quality and the power is transferred from the grid to the load. The system is termed as a smart as it is able to perform both modes automatically sensing the PV power and is capable of multidirectional power flow. The experimental validation is carried out on a developed prototype in the laboratory under varying modes.**

Keywords*— *PV-DSTATCOM, DSTATCOM, RZA and Power Quality.

I. INTRODUCTION

THE rising concern to explore for the substitute energy sources which are free from greenhouse emissions and are climate friendly, sustainable, pollution free have emerged renewable energy sources as a promising alternative. The incentives are being provided by many countries to offset the conventional generation through fossil fuels and to aid the paradigm shift towards generation through renewable energy sources. To have a sustainable climate friendly environment, the research is taking place to integrate large number of renewable energy sources in range of 3-50 kW with the grid. The grid connected renewable energy systems have the potential to improve system power quality, global warming and are capable of multidirectional power flow at the point of common coupling (PCC) [1-3].

Renewable energy systems including solar PV (Photovoltaic) have gained wide acceptance because the solar PV energy is a free source of energy and it is readily available [4]. The single stage topology which directly connects the PV system with the grid using a converter and the double stage topology which connects the PV system with a converter to the grid using a boost converter have been widely discussed in the literature [5] to integrate PV system with the electrical grid. However, the single stage topology is favored as the requirement of a DC-DC boost converter is eliminated, which reduces cost as well as it improves the system efficiency. The converter with PV array along with an active filter feature known as PV-DSTATCOM (PV- Distribution Static Compensator), is required to convert the DC voltage into AC and to improve the power quality by limiting harmonic distortions, to compensate the reactive power and to balance the power in all the three phases in the distribution system [6]. Moreover, a nonlinear relationship exists between PV voltage and current. Therefore, there is a particular value of voltage and current at which maximum power can be obtained from a PV array [7]. Various maximum power point tracking (MPPT) techniques have been reported such as hybrid fractional open-circuit voltage- current sensorless method [8], adaptive perturb and observe [9], grey wolf optimization technique [10], neural network [11] etc.

The rising energy demand, outages, high penetration of nonlinear loads with aging grid have possessed serious challenges for the grid [1]. In order to mitigate these problems, a smart PV-DSTATCOM system is proposed in this work which acts as an active filter and is able to nullify the effect of nonlinear load currents, to regulate the DC-link voltage, to improve the power factor of the grid and it is capable of multidirectional power flow. The proposed system is able to work into two modes PV-DSTATCOM and DSTATCOM and automatically perform two modes sensing the PV power. An optimal scheduling strategy can be designed based on forecasting so that the generation through fossil fuels can be minimized [12].The PV-DSTACOM offers the advantages of DSTATCOM, improves current quality problems and also transfers power to the load reducing the generation requirement through the conventional sources. If the power is available in excess multidirectional power flow, it can take place and the power is fed both to the grid and the load. However, when the solar PV power is not available, the system automatically performs in DSTATCOM mode and the power is fed to the load from the grid and the converter system. It acts as DSTATCOM for improving the power quality. The efficiency of a DSTATCOM control algorithm depends upon its effectiveness in extracting the reference current signals. Many control techniques such as SRF (Synchronous Reference Frame), IRPT (Instantaneous Reactive Power Theory), hybrid LMS-LMF (Least Mean Square-Least Mean Fourth), and leaky LMS current control have been studied in the literature [13-16] which use filters to obtain the reference current signals from the load currents. Phase locked loops have also been used to extract the reference current signals. However, intelligent adaptive techniques such as Adaline based LMS, LMF and variable forgetting factor recursive least squares have gained prominence for the control of PV-DSTATCOM. They provide good transient response than the conventional controls as the parameters are automatically adjusted according to the system dynamics and are easy to implement with basic mathematical operations. Singh. et.al. [15-16] have provided a comparison between SRF, IRPT and Adaline based LMS algorithm and it is highlighted that the Adaline based adaptive algorithm has a good performance as the weights are calculated online and has

Manuscript received June 26, 2016; revised October 18, 2016; accepted December 7, 2016. This work was supported by the Department of Science and Technology, Government of India project under Grant RP02583.
Paper no. TSG-00852-2016.

Bhim Singh and Ikhlaq Hussain are with the Department of Electrical Engineering, Indian Institute of Technology Delhi, New Delhi, India (e-mail: bhimsingh7nc@gmail.com; ikhlaqiitd@gmail.com).

Maulik Kandpal is with the Department of Electrical Engineering, Arizona State University, Tempe, Arizona, U.S. (e-mail: Maulik.kandpal@gmail.com).

1949-3053 (c) 2016 IEEE. Personal use is permitted, but republication/redistribution requires IEEE permission. See http://www.ieee.org/publications_standards/publications/rights/index.html for more information.

This article has been accepted for publication in a future issue of this journal, but has not been fully edited. Content may change prior to final publication. Citation information: DOI 10.1109/TSG.2016.2645600, IEEE Transactions on Smart Grid

a good dynamic performance. Kumar et. al. [17] have proposed an alternative way to extract reference current signals using enhanced phase locked loop instead of unit templates. Badoni et. al. [18] have proposed an adaptive variable forgetting factor RLS (Recursive Least Square) technique and compared it with fixed step RLS and variable step LMS. It is highlighted that the proposed RLS technique offers fast convergence and robustness. In this paper, an adaptive reweighted zero-attracting (RZA) control algorithm is used to extract the reference grid currents. The RZA control incorporates the l1 relaxation, widely discussed in the compressive sensing to improve the performance of the adaptive control which generates a zero attractor in the adaptive iteration and reduces the mean square error further in comparison to the normal LMS control providing with a good steady state and transient responses. Moreover, the use of reweighted zero attractor improves the filtering process and provides accurate reference signals [19]. The performance of the experimental system is evaluated on a developed prototype in the laboratory.

II. System Topology And Control Architecture

The proposed system consists of a 5.35 kW PV array tied to the three phase AC grid feeding linear and nonlinear loads with ripple filters as shown in Fig.1. The parameters of the KCG200GT PV array at nominal operating conditions have been used to model the required PV array as reported in [20]. To get a solar PV array of power 5.35 kW with array voltage (V_{pv}) as 340 V, the number of PV modules in parallel and series are set as 2 and 13, respectively in the solar PV array simulator ETS60017DPVF.

The proposed adaptive RZA control algorithm as shown in Fig. 2, is used to control the PV grid tied system with DSTATCOM capabilities described in this section. Fig. 3 shows flowchart for the operation of PV-DSTATCOM system.

The sensed two PCC line voltages (v_{ab} and v_{bc}) are used to calculate the phase voltages at PCC and their peak amplitude (V_t) [13] is expressed as,

$$v_a = \frac{2v_{ab} + v_{bc}}{3} \quad ; \quad v_b = \frac{-v_{ab} + v_{bc}}{3} \quad ; \quad v_c = \frac{-v_{ab} - 2v_{bc}}{3} \tag{1}$$

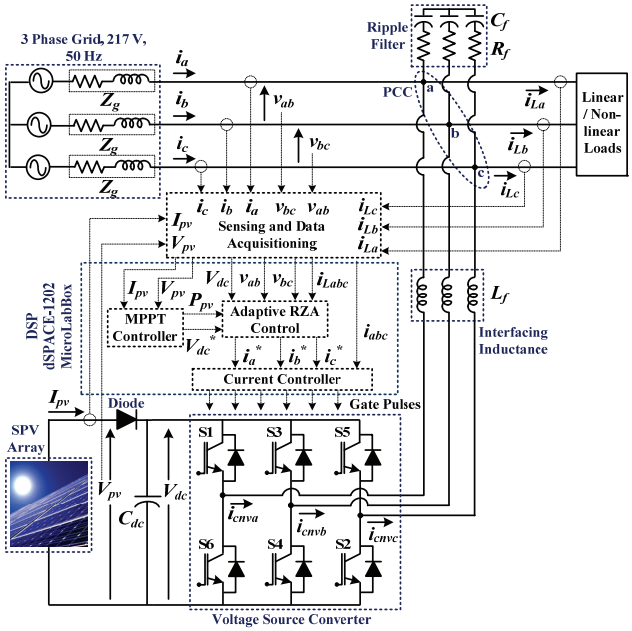

Fig. 1 Schematic of the proposed system topology

$$V_t = \sqrt{\frac{2}{3}(v_a^2 + v_b^2 + v_c^2)} \tag{2}$$

The in-phase unit and quadrature templates are evaluated as,

$$u_{pa} = \frac{v_a}{V_t} \quad ; \quad u_{pb} = \frac{v_b}{V_t} \quad ; \quad u_{pc} = \frac{v_c}{V_t} \tag{3}$$

$$u_{qa} = -\frac{u_{pb}}{\sqrt{3}} + \frac{u_{pc}}{\sqrt{3}}, u_{qb} = \frac{\sqrt{3}u_{pa}}{2} + \frac{(u_{pb} - u_{pc})}{2\sqrt{3}}$$
$$u_{qc} = -\frac{\sqrt{3}u_{pa}}{2} + \frac{(u_{pb} - u_{pc})}{2\sqrt{3}} \tag{4}$$

The DC voltage error (V_{de}) is estimated as the difference between the reference DC bus voltage (V_{dc}^*) achieved from the P&O MPPT and the sensed DC voltage (V_{dc}). The hill climbing approach of P&O works on the perturbation of voltage and observing the sign for the power and subsequently decides the nature for next perturb to reach the maximum power point. The error at the r[th] sampling instant is given as,

$$V_{de}(r) = V_{dc}^*(r) - V_{dc}(r) \tag{5}$$

The active loss component (w_{cp}) which is regulating the DC bus voltage (when irradiance level changes or load unbalancing takes place) is estimated by using V_{de} and a PI (Proportional Integral) controller gains (K_{id} and K_{pd} are integral and proportional gains) as,

$$w_{cp}(r+1) = w_{cp}(r) + K_{pd}(v_{de}(r+1) - v_{de}(r)) + K_{id}v_{de}(r+1) \tag{6}$$

Using Bode diagram, the stability analysis of the proposed system is carried out for DC bus voltage control. The system transfer function ($G_S(s)$ is evaluated as,

$$G_S(s) = G_P(s) * G_C(s) = \left[\frac{1}{sC_{dc}} * \left(k_{pd} + \frac{K_{id}}{s}\right)\right] \tag{7}$$

Where $G_p(s)$ is the plant transfer function and $G_C(s)$ is the PI voltage controller transfer function.

The Bode diagram is plotted for $G_S(s)$ as shown in Fig. 4 for system parameters as given in Appendix. It is seen from the Bode diagram of the system, the system is stable with phase and gain margin in the stable region.

Likewise, to regulate the PCC voltages (when irradiance level changes or load unbalancing takes place), the voltage error ($V_{te}(n)$) is fed to another PI controller. The error and reactive loss component (w_{cq}) at the r[th] sampling instant is evaluated as,

$$V_{te}(r) = V_t^*(r) - V_t(r) \tag{8}$$

$$w_{cq}(r+1) = w_{cq}(r) + K_{pt}(v_{te}(r+1) - v_{te}(r)) + K_{it}v_{te}(r+1) \tag{9}$$

Where, K_{it} and K_{pt} are integral and proportional gains used in this PI controller.

For an improved performance as irradiance level changes, the PV feed forward term from the solar PV array is estimated as,

$$w_{pv}(r) = 2P_{pv}(r)/(3V_t) \tag{10}$$

Where, P_{pv} is the extracted PV power.

The weight of fundamental active component of the load current of phase 'a' under steady state and dynamic conditions (when load unbalancing takes place) is evaluated as,

$$\mathbf{w_{pa}(r+1) = w_{pa}(r) - k_a \frac{\rho\, \mathrm{sgn}(w_{pa}(r))}{1 + \varepsilon\, |w_{pa}(r)|} + \mu\, e_{pa}(r)\, u_{pa}} \tag{11}$$

1949-3053 (c) 2016 IEEE. Personal use is permitted, but republication/redistribution requires IEEE permission. See http://www.ieee.org/publications_standards/publications/rights/index.html for more information.

This article has been accepted for publication in a future issue of this journal, but has not been fully edited. Content may change prior to final publication. Citation information: DOI 10.1109/TSG.2016.2645600, IEEE Transactions on Smart Grid

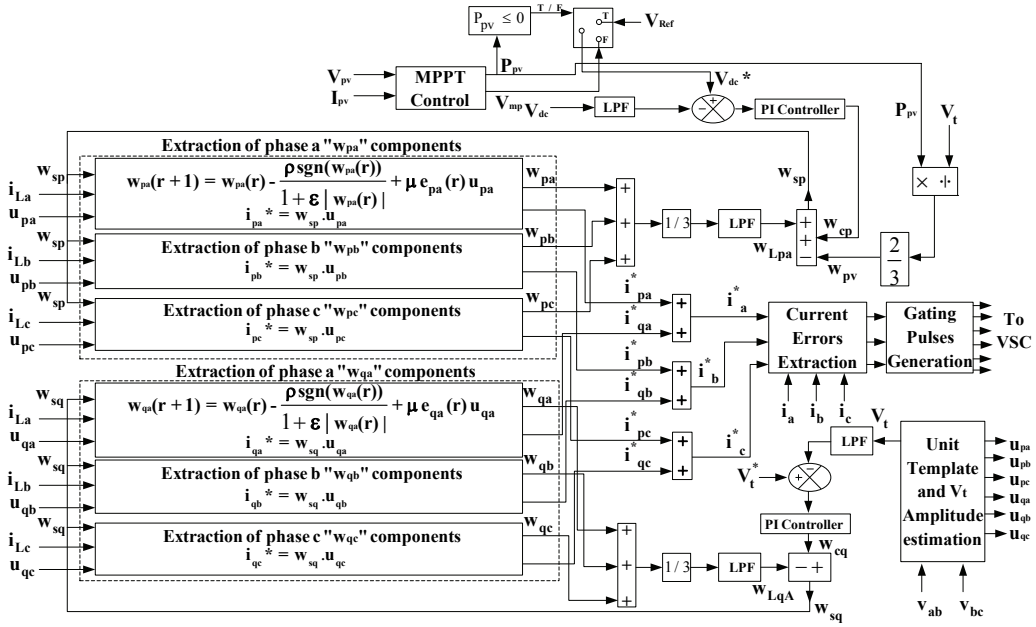

Fig. 2 Control architecture of the adaptive RZA based control with MPPT

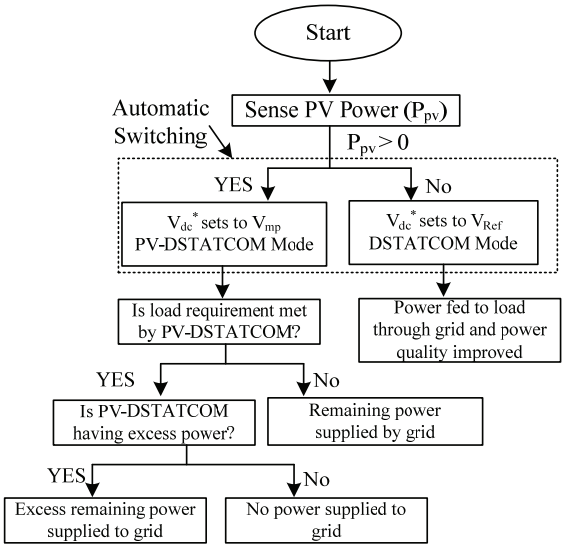

Fig. 3 Flowchart showing operation of PV-DSTATCOM System

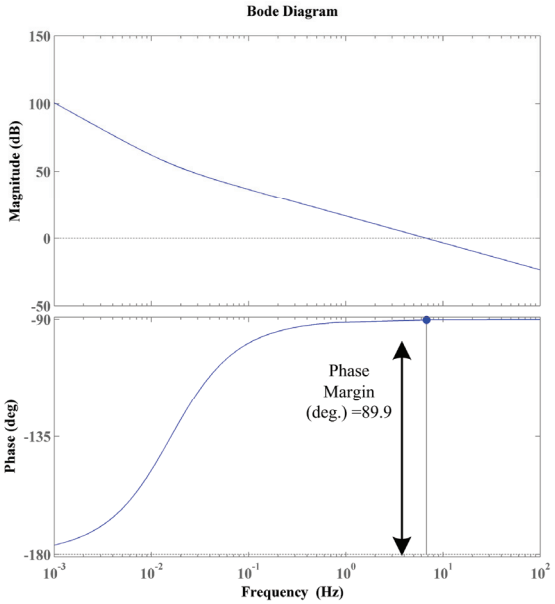

Fig. 4 Stability analysis of the proposed system using Bode diagram

Where, $e_{pa}(r) = i_{La}(r) - u_{pa}(r) \times w_{pa}(r)$, (12)

e_{pa} is the active error in the load component, ρ is a constant to control strength of zero attractor, k_a is the reweighted zero attractor term, μ is the convergence factor, sgn is the signum function, ε is a constant, $w_{pa}(r)$, $i_{La}(r)$ and $u_{pa}(r)$ are the weight of reference active component, load current and in-phase unit template of phase 'a' at the r^{th} instant. This relation (11) is similar to LMS control with an extra term k_a which improves convergence, and the steady state and transient responses of the adaptive control [19].

Likewise, the weights of fundamental active components ($w_{pb}(r)$, $w_{pc}(r)$) of the nonlinear load currents and adaptive component errors of other two phases 'b' and 'c' under steady state and dynamic conditions (when load unbalancing takes place) are expressed as,

$$w_{pb}(r+1) = w_{pb}(r) - \frac{\rho\,\mathrm{sgn}(w_{pb}(r))}{1+\varepsilon\,|\,w_{pb}(r)\,|} + \mu\, e_{pb}(r)\, u_{pb} \quad (13)$$

$$e_{pb}(r) = i_{Lb}(r) - u_{pb}(r) \times w_{pb}(r) \quad (14)$$

$$w_{pc}(r+1) = w_{pc}(r) - \frac{\rho\,\mathrm{sgn}(w_{pc}(r))}{1+\varepsilon\,|\,w_{pc}(r)\,|} + \mu\, e_{pc}(r)\, u_{pc} \quad (15)$$

$$e_{pc}(r) = i_{Lc}(r) - u_{pc}(r) \times w_{pc}(r) \quad (16)$$

Likewise, the weight of the fundamental reactive part of the nonlinear load current of phase 'a' under steady state and dynamic conditions (when load unbalancing takes place) is expressed as,

$$w_{qa}(r+1) = w_{qa}(r) - \frac{\rho\,\mathrm{sgn}(w_{qa}(r))}{1+\varepsilon\,|\,w_{qa}(r)\,|} + \mu\, e_{qa}(r)\, u_{qa} \quad (17)$$

$e_{qa}(r) = i_{La}(r) - u_{qa}(r) \times w_{qa}(r)$ is the reactive error.

Where, $w_{qa}(r)$, $i_{La}(r)$ and $u_{qa}(r)$ are the weight of reference reactive component, load current and quadrature unit template of phase 'a' at the r^{th} instant.

Likewise, the weights of the fundamental reactive components (($w_{qb}(r)$, $w_{qc}(r)$) of the nonlinear load currents and adaptive component errors of other two phases 'b' and 'c' under steady state and dynamic conditions (when load unbalancing takes place) are written as,

1949-3053 (c) 2016 IEEE. Personal use is permitted, but republication/redistribution requires IEEE permission. See http://www.ieee.org/publications_standards/publications/rights/index.html for more information.

This article has been accepted for publication in a future issue of this journal, but has not been fully edited. Content may change prior to final publication. Citation information: DOI 10.1109/TSG.2016.2645600, IEEE Transactions on Smart Grid

$$\mathbf{w_{qb}(r+1) = w_{qb}(r) - \frac{\rho\, sgn(w_{qb}(r))}{1+\varepsilon\,|\,w_{qb}(r)\,|} + \mu\, e_{qb}(r)\, u_{qb}} \quad (18)$$

$$e_{qb}(r) = i_{Lb}(r) - u_{qb}(r) \times w_{qb}(r) \quad (19)$$

$$\mathbf{w_{qc}(r+1) = w_{qc}(r) - \frac{\rho\, sgn(w_{qc}(r))}{1+\varepsilon\,|\,w_{qc}(r)\,|} + \mu\, e_{qc}(r)\, u_{qc}} \quad (20)$$

$$e_{qc}(r) = i_{Lc}(r) - u_{qc}(r) \times w_{qc}(r) \quad (21)$$

The active weight component (w_{sp}) of reference grid currents under steady state and dynamic conditions (when irradiance level changes or load unbalancing takes place) is expressed as,

$$w_{sp} = w_{LpA} + w_{cp} - w_{pv} \quad (22)$$

$$\text{Where, } w_{LpA} = (w_{pa} + w_{pb} + w_{pc})/3 \quad (23)$$

Moreover, the reference active grid currents under steady state and dynamic conditions (when irradiance level changes or load unbalancing takes place) are evaluated as,

$$i^*_{pa} = w_{sp}.u_{pa} \quad ; \quad i^*_{pb} = w_{sp}.u_{pb} \quad ; \quad i^*_{pc} = w_{sp}.u_{pc} \quad (24)$$

Likewise, the total reactive weight component (w_{sq}) of reference grid currents under steady state and dynamic conditions (when irradiance level changes or load unbalancing takes place) is expressed as,

$$w_{sq} = w_{cq} - w_{LqA} \quad (25)$$

$$\text{Where, } w_{LqA} = (w_{qa} + w_{qb} + w_{qc})/3 \quad (26)$$

Likewise, the reference reactive grid currents under steady state and dynamic conditions (when irradiance level changes or load unbalancing takes place) are evaluated as,

$$i^*_{qa} = w_{sq}.u_{qa} \quad ; \quad i^*_{qb} = w_{sq}.u_{qb} \quad ; \quad i^*_{qc} = w_{sq}.u_{qc} \quad (27)$$

So, the total reference three-phase grid currents under steady state and dynamic conditions (when irradiance level changes or load unbalancing takes place) are evaluated as,

$$i^*_{sa} = i^*_{pa} + i^*_{qa}\,;\; i^*_{sb} = i^*_{pb} + i^*_{qb}\,;\; i^*_{sc} = i^*_{pc} + i^*_{qc} \quad (28)$$

For generation of the gate pulses for switching of VSC (Voltage Source Converter), the difference of the reference grid currents and the sensed grid currents is passed through the hysteresis regulator to generate pulses for the converter.

III. Results And Discussion

A prototype of a grid tied PV system with the DSTATCOM capabilities using a RZA adaptive control algorithm is implemented. An AMETEK make photovoltaic array simulator (ETS60017DPVF) is used to emulate the characteristics of the PV array. The control algorithm discussed in Section II is realized using a DSP (dSPACE-1202), Hall-effect voltage sensors (LV25P) and current sensors (LA55P). The opto-coupler circuits (6N136) are used to provide necessary optical isolation between the VSC and the DSP signals. Test results have been recorded using four channel an Agilent make DSO (DSO7014A) and a power analyzer (Fluke make, model: 43B). The detailed data of experimental system are given in Appendix.

A. Performance of PV-DSTATCOM System under Linear Loads

The steady state behaviour of the proposed PV grid tied system under linear loads, a combination of resistance and inductance is depicted in Figs. 5 (a-l). Figs. 5 (a-c) show the waveforms of PCC line voltage (v_{ab}) with grid currents (i_c, i_a and i_b) of each phase, respectively. Fig. 5 (d) shows the grid power along with the power factor. The negative notation for the grid power depicts that the PV-DSTATCOM system is in operation and the power is being fed to the grid. Moreover, it is observed that the power factor of the grid is maintained at unity. Figs. 5 (e-g) show the waveforms of PCC line voltage (v_{ab}) with load currents (i_{Lc}, i_{La} and i_{Lb}) of each phase, respectively. Fig. 5 (h) shows the load power along with power factor. It is observed that the PV-DSTATCOM system is able to improve the power factor from 0.72 to unity. Figs. 5 (i-k) show the waveforms of v_{ab} with PV-VSC currents (i_{invc}, i_{inva} and i_{invb}) of each phase, respectively. Fig. 5 (l) shows the PV-VSC power. The positive notation for VSC power indicates that the PV-VSC is supplying power to both the load and the grid.

B. Response of PV-DSTATCOM System under Nonlinear Loads

The response of the proposed PV-DSTATCOM grid tied system under nonlinear loads is depicted in Figs. 6 (a-h) and Figs. 7 (a-b). Fig. 6 (a) shows the waveforms of v_{ab} and i_c. Fig. 6 (b) depicts the THD (Total Harmonic Distortion) of i_c which is 2.7 % and within limits of an IEEE-519 standard [21]. Fig. 6 (c) shows the waveforms of v_{ab} and i_{Lc}. Fig. 6 (d) depicts the THD of the load current (i_{Lc}) which is 26.8 %. Fig. 6 (e) shows the waveforms of PCC line voltage (v_{ab}) and VSC current (i_{invc}). Finally, Figs. 6 (f-g) depict the grid power, load power

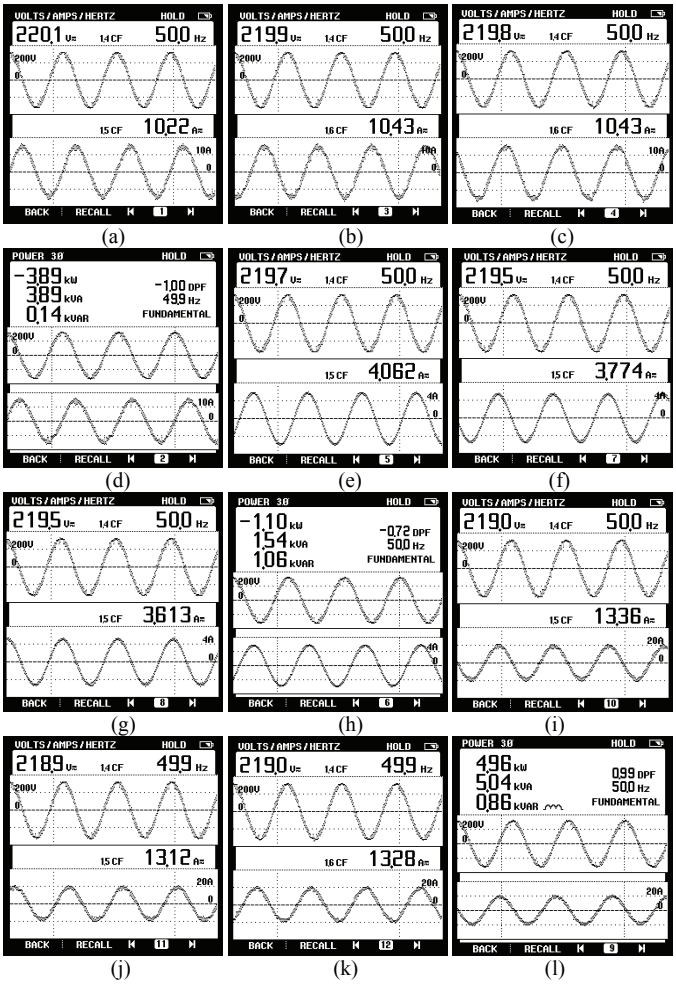

Fig. 5 Steady state response of the PV-DSTATCOM grid tied system with linear loads (a) v_{ab} with i_c (b) v_{ab} with i_a (c) v_{ab} with i_b (d) Grid Power with i_c (e) v_{ab} with i_{Lc} (f) v_{ab} with i_{La} (g) v_{ab} with i_{Lb} (h) Load Power with i_{Lc} (i) v_{ab} with i_{invc} (j) v_{ab} with i_{inva} (k) v_{ab} with i_{invb} (l) Converter Power with i_{invc}

1949-3053 (c) 2016 IEEE. Personal use is permitted, but republication/redistribution requires IEEE permission. See http://www.ieee.org/publications_standards/publications/rights/index.html for more information.

This article has been accepted for publication in a future issue of this journal, but has not been fully edited. Content may change prior to final publication. Citation information: DOI 10.1109/TSG.2016.2645600, IEEE Transactions on Smart Grid

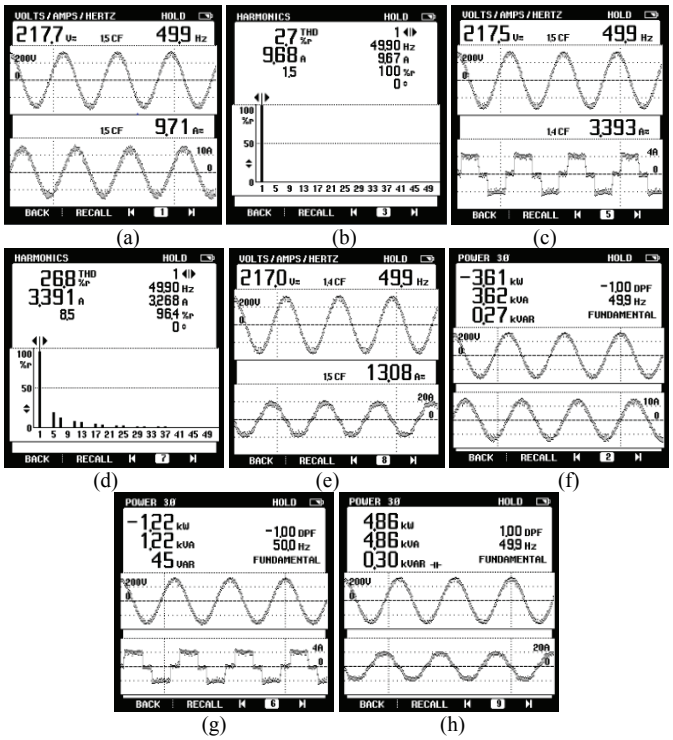

Fig. 6 Steady state responses of the PV-DSTATCOM grid tied system under nonlinear loads (a) v_{ab} with i_c (b) THD of i_c (c) v_{ab} with i_{Lc} (d) THD of i_{Lc} v_{ab} with i_{invc} (e-g) grid power, (h) load power and PV-VSC power.

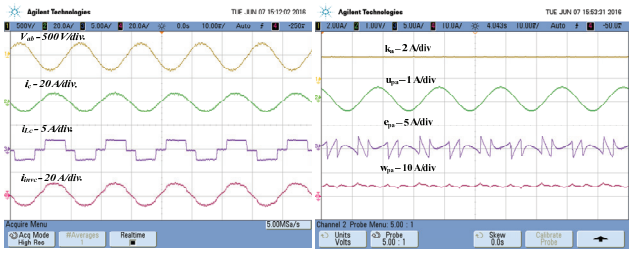

Fig. 7 (a-b) Steady state response of PV-DSTATCOM system at solar intensity of 1000 W/m^2

with negative notation showing that the PV array power is fed to the loads and the grid. Fig. 6 (h) shows PV-VSC power. Figs. 7 (a-b) show the waveforms of v_{ab}, i_c, i_{Lc}, i_{invc} and k_a (the reweighted zero attractor term), u_{pa} (the unit template for phase a), e_{pa} (the active error in the load component for phase a) and w_{pa} (the weight for reference active component for phase a) at a solar insolation of 1000 W/m^2.

C. Performance of PV-DSTATCOM System under Unbalanced Nonlinear Loads

Figs. 8 (a-b) depict the dynamic behaviour and the response of internal signals of the proposed system under an unbalanced load. When the load of phase 'a' is suddenly disconnected the response of v_{ab}, i_a, i_{La} and i_{inva} is shown in Fig. 8 (a). Similarly, Fig. 8 (b) shows the waveforms on sudden load addition in phase a. It is observed that even when the load is unbalanced, the grid current, i_a remains sinusoidal. Figs. 8 (c-d) show the response of phase b waveform when the load is suddenly disconnected and added in phase a, respectively where V_{dc} shows the DC-link voltage, i_b shows the grid current in phase b, i_{Lb} shows the load current waveform for phase b and i_{invb} is the converter current of phase b. Figs. 8 (e-f) show the internal signals of the proposed algorithm when the load of phase 'a' is suddenly disconnected and reconnected, respectively in the system. In these figures, waveforms of the active power loss component (w_{cp}), the component of feed forward term (w_{pv}), the weight of load component (w_{Lpa}), the total active weight component (w_{sp}), k_a, u_{pa}, e_{pa} and w_{pa} are shown. It is observed that on load disconnection, the error and the weight component for phase are reduced to zero. Similarly, Figs. 8 (g-h) show the waveforms for load addition in phase a.

D. Performance of PV-DSTATCOM System under Variable Solar Insolation

Figs. 9 (a-b) show the dynamic behaviour of PV-DSTATCOM grid tied system under varying solar irradiance. Fig. 9 (a) shows the variation in DC-link voltage (V_{dc}), PV array current (I_{pv}), converter current of phase a (i_{inva}) and grid current of phase a (i_a) on changing the solar insolation (1000 W/m^2 to 600 W/m^2). It is observed that with a decrease in the solar intensity, there is a decrease in I_{pv}, i_{invc} and i_c. However, V_{dc} remains constant with minor fluctuation during an insolation change and regains its value after few cycles.

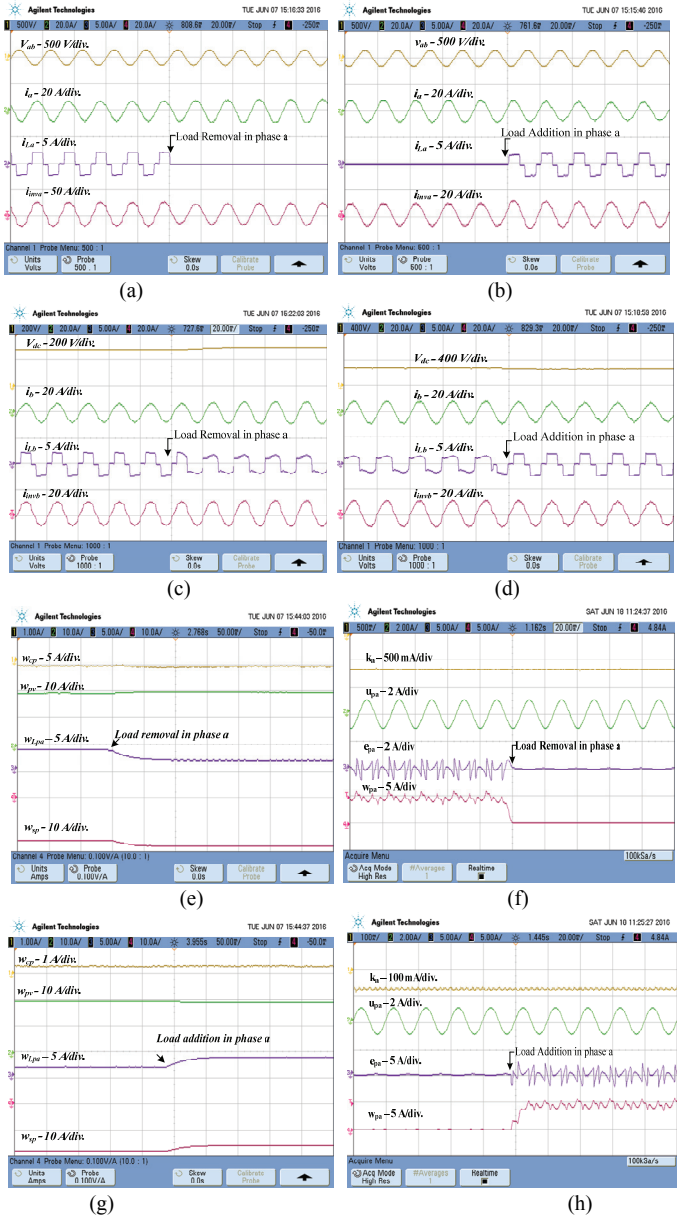

Fig. 8 (a-b) Dynamic responses of the PV-DSTATCOM grid tied system under unbalanced nonlinear load in phase a (c-d) Dynamic responses of the PV-DSTATCOM grid tied system under unbalanced nonlinear load in phase a on phase c (e-h) Response of internal signals of control under unbalanced nonlinear load.

1949-3053 (c) 2016 IEEE. Personal use is permitted, but republication/redistribution requires IEEE permission. See http://www.ieee.org/publications_standards/publications/rights/index.html for more information.

This article has been accepted for publication in a future issue of this journal, but has not been fully edited. Content may change prior to final publication. Citation information: DOI 10.1109/TSG.2016.2645600, IEEE Transactions on Smart Grid

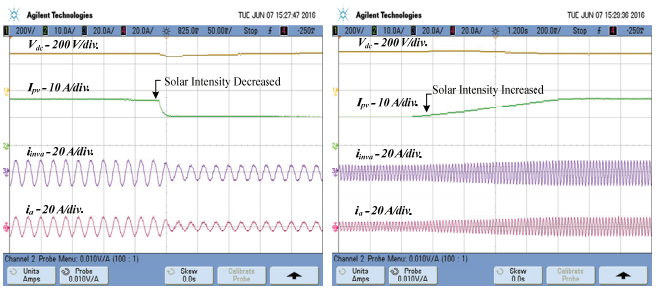

(a) (b)

Fig. 9 Dynamic performance of the PV-DSTATCOM grid tied system (a) decrease in solar intensity (b) increase in solar intensity.

Similarly, Fig. 9 (b) shows the similar waveforms for an increase in solar irradiance (600 W/m^2 to 1000 W/m^2). Figs. 10 (a-b) show the MPPT performance of the PV array which is nearly 100% at solar intensity level of 600 W/m^2 and 1000 W/m^2 respectively.

E. Performance under Change from PV-DSTATCOM mode to DSTATCOM Mode and Vice Versa

Fig. 11 (a) shows the behaviour of the PV-DSTATCOM system on the shifting from PV-DSTATCOM to DSTATCOM mode which occurs during less solar intensity or at night conditions when the PV array is not functioning. It is observed that after transition, V_{dc} remains constant and tracks the set reference DC-link voltage for DSTATCOM mode which earlier has been tracking the reference voltage, V_{dc}^* obtained from the MPPT controller. I_{pv} gets zero and the converter current waveform is changed as the active current provided by PV array is no longer available. However, the grid current (i_c) remains sinusoidal with the reversal in the grid current direction during transition because in PV-DSTATCOM mode and the PV system has been supplying the power to both the load and the grid. However, in DSTATCOM mode, the grid supplies the power to loads. Fig. 11 (b) shows the internal signals for a change from PV-DSTATCOM to DSTATCOM mode, where w_{cp} is the waveform of the active loss component, w_{pv} the component of feed forward term, w_{Lpa} the weight of load component and w_{sp} the total active weight component.

Fig. 11 (c) shows the transition from DSTATCOM to PV-DSTATCOM mode. It is observed that V_{dc} is maintained at its set value. There is a ramp increase in the PV array current and the steady state condition is obtained and the converter current (i_{inva}) and grid current are increased (i_a) as an active current component is provided by the PV array. Fig. 11 (d) shows the internal signals for a change from DSTATCOM to PV-DSTATCOM mode.

F. Performance of Comparison of Adaptive RZA Control Algorithm with Existing Control Algorithms

The performance comparison of proposed adaptive RZA control algorithm with existing SRF and LMS control algorithms are given in Table I. The adaptive RZA control algorithm has low complexity and high DSP speed than SRF control algorithm due to less number of computations of the control. The proposed control algorithm has better accuracy, low oscillations and reduced mean square error (MSE) than LMS control algorithm. Due to less MSE, the system converges fast and has better performance under dynamicconditions. Due to low oscillations, the system has less THD in the grid current and voltage.

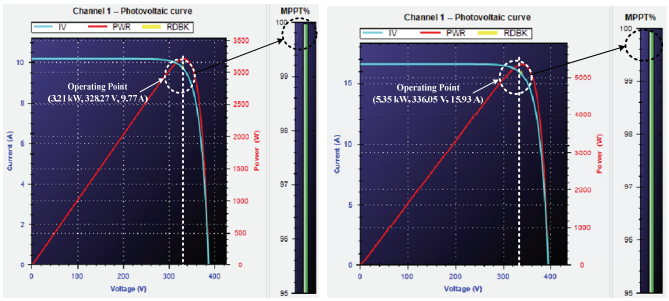

(a) (b)

Fig. 10 MPPT performance of PV array at solar intensity of (a) 600 W/m^2 (b) 1000

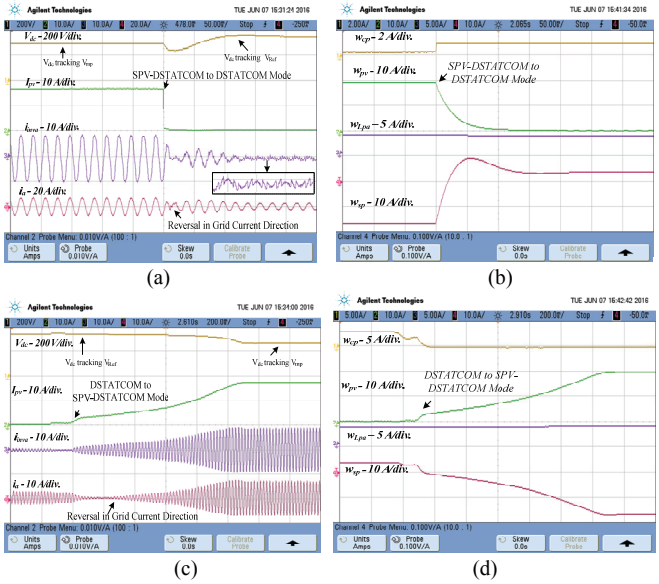

(a) (b)

(c) (d)

Fig. 11 Response of the PV-DSTATCOM grid tied system (a-b) Change from PV-DSTATCOM to DSTATCOM mode (c-d) Change from DSTATCOM to PV-DSTATCOM mode

TABLE I

COMPARISON OF PROPOSED ADAPTIVE RZA CONTROL ALGORITHM WITH EXISTING CONTROL ALGORITHMS

Parameter	Conventional control algorithms		Proposed control (RZA)
	SRF	LMS	
Filter type	Time-domain PLL-based	Adaptive filter	Adaptive filter
Complexity	High	Low	Low
Accuracy	Better	Good	Better
Static error	NA	More	Less
DSP speed	Low	High	High
Oscillations	Medium	High	Low
MSE	NA	37.6	27.24
Number of computations	More	Less	Less
Sampling time (T_s)	40 µs	30 µs	30 µs
Settling time	0.15 s	0.1 s	0.091 s

IV. CONCLUSION

The proposed grid tied smart PV-DSTATCOM system has been implemented in the laboratory using an adaptive RZA control algorithm with P & O based MPPT technique for a three phase system to improve power quality and to support the three phase AC grid by supplying the power both to the grid and the connected loads. The control strategy has been presented for the three-phase grid-tied single stage PV system with DSTATCOM capabilities using adaptive RZA technique for extracting reference grid currents and an P&O-MPPT

1949-3053 (c) 2016 IEEE. Personal use is permitted, but republication/redistribution requires IEEE permission. See http://www.ieee.org/publications_standards/publications/rights/index.html for more information.

This article has been accepted for publication in a future issue of this journal, but has not been fully edited. Content may change prior to final publication. Citation information: DOI 10.1109/TSG.2016.2645600, IEEE Transactions on Smart Grid

control is used to tack maximum power at all instants. The use of RZA strategy has presented the good steady state and transient responses and the experimental results have justified the dual capability of the system to work in PV-DSTATCOM and DSTATCOM modes. The proposed system has worked well under load unbalance and it has maintained the power quality. Moreover, the presented system has conformed to an IEEE-519 standard for harmonics and IEEE-1547 standard for PV system interfaced to the grid.

V. Acknowledgment

The authors are highly thankful to Department of Science and Technology, Govt. of India, for supporting this project under Grant Number: RP02583.

Appendices

Experimental System Parameters: PV simulator array OC voltage, V_{OCN} = 394.80 V; array SC current, I_{SCN} = 16.62 A; array power, P_{MPP} = 5.35 kW; DC Bus Voltage, V_{Ref} = 380 V; Interfacing inductor, L_f = 2.9 mH; DC Bus Capacitor, C_{dc} = 2350 μF; sampling time, T_s = 30 μs; grid voltage, V_{LL} = 220V (rms) ; ripple filter, R_f = 5 Ω and C_f = 10 μF, DC PI controller, K_{pd} = 0.1 and K_{id} = 0.01; Nonlinear load: 3-phase diode bridge with a 1.10 kW load, Control parameters : μ=0.054, ε=10.2, ρ=0.004.

References

[1] G. M. Shafiullah, M. T. Amanullah, A. B. M. Shawkat Ali, P. Wolfs and M. T. Arif, *Smart Grids: opportunities, developments and trends*, Springer, London, 2013.

[2] S. J. Steffel, P. R. Caroselli, A. M. Dinkel, J. Q. Liu, R. N. Sackey and N. R. Vadhar, "Integrating solar generation on the electric distribution grid," *IEEE Trans. Smart Grid*, vol. 3, no. 2, pp. 878-886, June 2012.

[3] T. Wang, D. O'Neill and H. Kamath, "Dynamic control and optimization of distributed energy resources in a microgrid," *IEEE Trans. Smart Grid*, vol. 6, no. 6, pp. 2884-2894, Nov. 2015.

[4] K. Jager, O. Isabella, A. H. M. Smets, R. A. C. M. M. Van Swaaij and M. Zeman, *Solar energy fundamentals, technology and systems*, Delft University of Technology, 2014.

[5] T. F. Wu, C. H. Chang, L. C. Lin and C. L. Kuo, "Power loss comparison of single- and two-stage grid-connected photovoltaic systems," *IEEE Trans. Energy Convers*., vol. 26, no. 2, pp. 707-715, June 2011.

[6] R. Agarwal, I. Hussain and B. Singh, "LMF based control algorithm for single-stage three-phase grid integrated solar PV system," *IEEE Trans. Sus. Energy*, vol. 7, no. 4, pp. 1379-1387, Oct. 2016.

[7] Bidyadhar Subudhi and Raseswari Pradhan, "A comparative study on maximum power point tracking techniques for photovoltaic power systems," *IEEE Transactions Sus. Energy*, vol.4, no.1, pp.89-98, January 2013.

[8] C. C. Hua, Y. H. Fang and W. T. Chen, "Hybrid maximum power point tracking method with variable step size for photovoltaic systems," *IET Renew. Pow. Gen.*, vol. 10, no. 2, pp. 127-132, Feb. 2016.

[9] S. K. Kollimalla and M. K. Mishra, "A novel adaptive P&O MPPT algorithm considering sudden changes in the irradiance," *IEEE Trans. Energy Conversion*, vol. 29, no. 3, pp. 602-610, Sept. 2014.

[10] S. Mohanty, B. Subudhi and P. K. Ray, "A new MPPT design using grey wolf optimization technique for photovoltaic system under partial shading conditions," *IEEE Trans. Sustainable Energy*, vol. 7, no. 1, pp. 181-188, Jan. 2016

[11] L. M. Elobaid, A. K. Abdelsalam and E. E. Zakzouk, "Artificial neural network-based photovoltaic maximum power point tracking techniques: a survey," *IET Renew. Pow. Gen.*, vol. 9, no. 8, pp. 1043-1063, Nov. 2015.

[12] S. S. Reddy and J. A. Momoh, "Realistic and transparent optimum scheduling strategy for hybrid power system," *IEEE Trans. Smart Grid*, vol. 6, no. 6, pp. 3114-3125, Nov. 2015.

[13] B. Singh, A. Chandra, and K. Al-Haddad, *Power quality: problems and mitigation techniques*, John Wiley & Sons Ltd., United Kingdom, 2015.

[14] M. Srinivas, I. Hussain and B. Singh, "Combined LMS-LMF based control algorithm of DSTATCOM for power quality enhancement in distribution system," *IEEE Trans. Ind. Electron*., vol. 63, no. 7, pp. 4160-4168, July 2016.

[15] B. Singh and J. Solanki, "A comparison of control algorithms for DSTATCOM," *IEEE Trans. Ind. Elec.*, vol. 56, no. 7, pp. 2738-2745, July 2009.

[16] S. R. Arya and B. Singh, "Performance of DSTATCOM using leaky LMS control algorithm," *IEEE Journal of Emerging and Selected Topics in Power Electronics*, vol. 1, no. 2, pp. 104-113, June 2013.

[17] S. Kumar and A. K. Verma, Ikhlaq Hussain and Bhim Singh, "Performance of grid interfaced SPV system under variable solar intensity," in *Proc. IEEE 6th India International Conference Pow. Electron.*, 8-10 Dec. 2014, pp.1-6.

[18] M. Badoni, A. Singh and B. Singh, "Variable forgetting factor recursive least square control algorithm for DSTATCOM," *IEEE Trans. on Pow. Deli.,* vol. 30, no. 5, pp. 2353-2361, Oct. 2015.

[19] Yilun Chen, Y. Gu and A. O. Hero, "Sparse LMS for system identification," in *Proc. IEEE Int. Conf. on Acoustics, Speech and Signal Processing*, 2009, pp. 3125-3128.

[20] M. G. Villalva, J. R Gazoli and E. R. Filho, "Comprehensive approach to modeling and simulation of photovoltaic arrays," *IEEE Trans. Pow. Elec.*, vol. 24, no. 5, pp. 1198-1208, May 2009.

[21] IEEE Recommended Practices and Requirement for Harmonic Control on Electric Power System, IEEE Std.519, 1992.

Bhim Singh (SM'99, F'10) was born in Rahamapur, Bijnor (UP), India, in 1956. He received his B.E. (Electrical) from University of Roorkee, India, in 1977 and his M. Tech. (Power Apparatus & Systems) and Ph.D. from the IIT Delhi, India, in 1979 and 1983, respectively. In 1983, he joined the Department of Electrical Engineering, University of Roorkee (Now IIT Roorkee), as a Lecturer. He became a Reader there in 1988. In December 1990, he joined the Department of Electrical Engineering, IIT Delhi, India, as an Assistant Professor, where he has become an Associate Professor in 1994 and a Professor in 1997. He has been Head of the Department of Electrical Engineering at IIT Delhi from July 2014 to August 2016. Presently, he is Dean, Academics at IIT Delhi. Prof. Singh has guided 65 Ph.D. dissertations, 161 M.E./M.Tech./M.S.(R) thesis. He has executed more than seventy five sponsored and consultancy projects.

His areas of research interest include PV grid interface systems, microgrid, power quality, PV water pumping systems, power electronics, electrical machines, drives, FACTS and HVDC systems.

Maulik Kandpal received the B.E. degree in electrical engineering from Delhi College of Engineering, India, in 2013, and is currently pursuing the M.S.E. degree in electrical engineering at Arizona State University, Tempe, AZ, USA. He has worked as a Research Assistant with Electrical Engineering, Indian Institute of Technology Delhi, New Delhi, India.

His research interests include renewable energy systems, power quality and power electronics.

Ikhlaq Hussain (S'14–M'15) was born in Doda, Jammu and Kashmir, India, in 1986. He received his B. E. (Electrical) from University of Jammu, Jammu, India, in 2009 and M. Tech. (Gold Medalist) in Electrical power System Management from the Jamia Millia Islamia (A Central University), New Delhi, India, in 2012. He is currently working toward his Ph.D. in the Department of Electrical Engineering, Indian Institute of Technology Delhi, New Delhi, India.

His areas of research interests include power quality, custom power devices, renewable energy systems and microgrid.

1949-3053 (c) 2016 IEEE. Personal use is permitted, but republication/redistribution requires IEEE permission. See http://www.ieee.org/publications_standards/publications/rights/index.html for more information.